Journal of Hazardous Materials 168 (2009) 997–1003

Contents lists available at ScienceDirect

Journal of Hazardous Materials

journal homepage: www.elsevier.com/locate/jhazmat

Electrochemical oxidation of an azo dye in aqueous media investigation of operational parameters and kinetics

J. Basiri Parsa*, M. Rezaei, A.R. Soleymani

Faculty of Chemistry, Bu-Ali Sina University, Hamedan 65178, Iran

ARTICLE INFO

Article history:
Received 26 January 2008
Received in revised form 6 January 2009
Accepted 24 February 2009
Available online 9 March 2009

Keywords:
Electrochemical oxidation
Direct blue 71
Decolorization
Kinetics

ABSTRACT

In this research two types of electrochemical reactors for the treatment of simulated wastewaters containing Direct blue 71 azo dye (DB71) were used: (1) Laboratory scale undivided electrolysis cell system (450 mL volume) with one 2 cm × 2 cm platinum plate as the anode placed in the middle of the cell and two 2 cm × 8 cm steel plates (SS-304) as cathodes placed in the sides of the cell 2 cm from the central anode. (2) Pilot scale reactor (9 L volume), equipped with two 3 cm × 23 cm stainless steel plates as anode and cathode, with distance of 3 cm apart. The influence of supporting electrolyte, applied voltage and pH were studied. The UV–vis spectra of samples during the electrochemical oxidation showed the rapid decolorization of the dye solution. During the process, the COD and current were measured in order to evaluate the degree of mineralization, energy consumption, current and anode efficiencies. The optimum supporting electrolyte and applied voltage were NaCl (5 g L^{-1}) and 15 V. Using the lab scale reactor resulted in complete decolorization and mineralization of the dye solutions after ca. 90 and 120 min, respectively. Similar results were obtained using the pilot plant reactor under the same conditions. The good fit of the data to pseudo-first-order kinetics for COD removal at all applied voltages (except 20 V) was taken as proof of the involvement of indirect oxidation pathways in the process.

1. Introduction

Azo dyes are among the major pollutants of wastewaters from textile industries; in many areas, these industries discharge wastewaters having strong color, variable pH and temperature, high COD and low biodegradability and therefore are difficult to treat satisfactorily [1]. The dyes are particularly important in wastewater treatment, and are stable under all usual environmental conditions (exposure to sunlight, water, soap, soil, etc.) and become more difficult to treat. Due to the stability of organic dyes, removal of color is therefore a challenge to both the textile industry and wastewater treatment facilities [2]. Dye containing wastewaters are usually treated by conventional methods such as biological oxidation [3], adsorption [4], or coagulation by aluminum or iron salts [5]. Because of the large variation in the composition of wastewaters from textile industries, most of these traditional methods are inadequate [6]. In recent years, there has been an increasing interest in the use of photocatalytic, electrochemical and combined methods for the treatment of wastewaters [7–10]. An important advantage of electrochemical oxidation is the potential to completely oxidize organic pollutants to CO_2 and H_2O and hence avoid the problem of contaminants being transferred from one phase to another. Also, the advantage of operation at room temperature and atmospheric pressure offered by electrochemical oxidation prevents volatilization and discharge of remaining wastes to the environment, as well as complete control of the reaction. In the work reported in this paper the electrochemical treatment of a simulated wastewater containing a stable azo dye, Direct blue 71 (DB71), was investigated. Experiments to determine the optimum treatment conditions were carried out in a laboratory scale undivided cell reactor and, in order to evaluate the scaling up potential of the electrochemical process, a pilot plant scale reactor.

2. Experimental

2.1. Reagents

All reagents were used as received without further purification. The azo dye DB71, $C_{40}H_{23}N_7Na_4O_{13}S_4$ (C.I no.: 34140, CAS no.: 4399-55-7, MW = 1029.9) was provided by Alvan Sabet company (Iran) with a purity of >99%. Fig. 1 shows the structure of this dye. Sulfuric acid and sodium hydroxide were used to adjust the pH of solution and sodium, potassium and calcium chlorides and sodium sulphate were used as supporting electrolytes these chemicals were purchased from Merck with purities of more than 99.5%.

* Corresponding author. Tel.: +98 811 8272072; fax: +98 811 8256711.
E-mail address: Parssa@basu.ac.ir (J.B. Parsa).

0304-3894/$ – see front matter © 2009 Elsevier B.V. All rights reserved.
doi:10.1016/j.jhazmat.2009.02.134

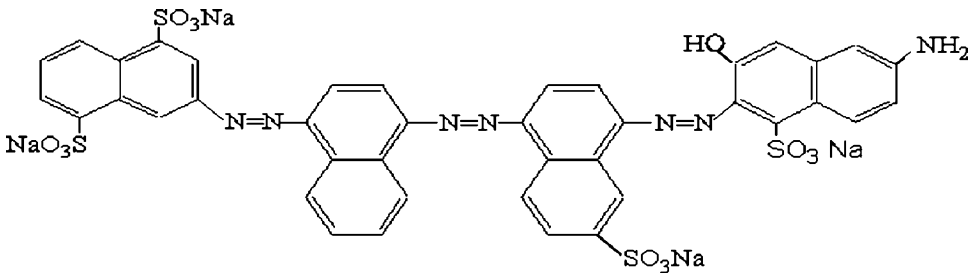

Fig. 1. Chemical structure of Direct blue 71.

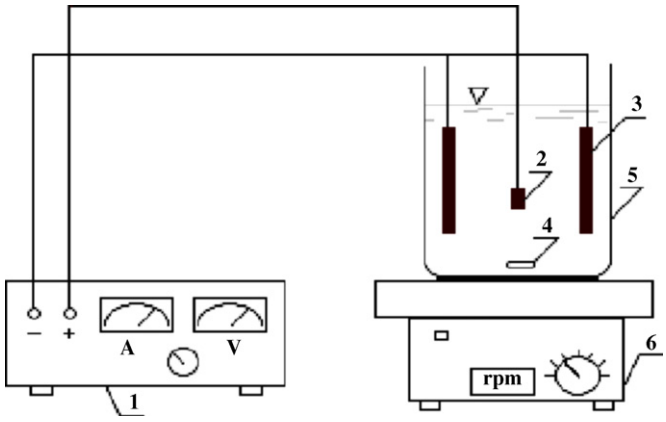

Fig. 2. The schematic view of the undivided lab electrolysis cell system: (1) supply source; (2) platinum anode; (3) steel cathode; (4) magnet; (5) electrolysis cell; (6) magnetic stirrer.

2.2. The reactors

Two types of electrochemical reactor were used. (1) Laboratory scale undivided electrolysis cell system (450 mL volume) with one 2 cm × 2 cm platinum plate as the anode placed in the middle of the cell and two 2 cm × 8 cm steel plates (SS-304) as cathodes placed in the sides of the cell 2 cm from the central anode. (2) Pilot scale reactor (9 L volume), equipped with two 3 cm × 23 cm dimension stainless steel plates as anode and cathode, 3 cm apart. Schematic representation of the reactors are presented in Figs. 2 and 3.

Table 1
The operative conditions of experiments.

Parameter	Value
DB71 initial concentration (mg L^{-1})	100
Electrolyte amount (g L^{-1})	5, 10, 20
Applied voltage (V)	5, 7.5, 10, 15, 20
pH	4, 7, 9
Temperature (°C)	25 (pilot), ambient (lab scale)
Time (min)	Up to 120

2.3. Procedure

In order to perform the experiments using the laboratory undivided electrolysis cell, the appropriate solutions, containing 100 mg L^{-1} of dye (about 10^{-4} M) and a known amount of supporting electrolyte, e.g. NaCl, KCl or Na_2SO_4, were prepared. The pH was adjusted to the desired value by means of a pH meter (JENWAY, UK-3010) using dilute H_2SO_4 or NaOH. The solution was then transferred to the reactor and after adjusting the temperature, the electrolysis process was initiated. During each experiment, mixing of the reactor contents was maintained to keep the solution homogenous and at a uniform temperature. In the pilot reactor the temperature was controlled between 20–25 °C by circulating cooling water, whilst the lab scale reactor experiments were carried out at ambient temperature. Samples were taken at regular time intervals. The operational conditions of the experiments are given in Table 1.

The concentration of the dye in each sample was analyzed with a UV–vis spectrophotometer (PerkinElmer, 55 OSE), measuring the absorbance at λ_{max} = 584 nm and using the appropriate calibration curve. It is noteworthy that the maximum wavelength and the

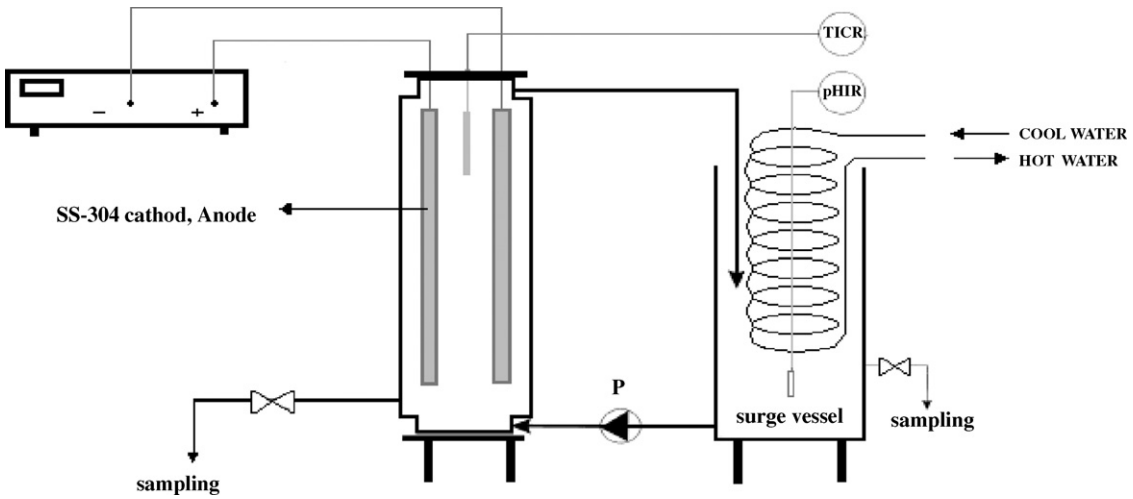

Fig. 3. The schematic view of Pilot scale reactor: P = direct current pump; pHIR = pH meter; TICR = temperature indicator controller recorder.

molar absorption coefficient of DB71 do not depend to any great extent on the pH of solution within the range of 4–10 [7]. Using this method, the degradation efficiency or conversion (X%) of DB71 can be obtained at any time, with respect to its initial concentration. This parameter is commonly used in degradation studies. As decolorization can be correlated with the modification of the dye's chemical structure but not with the reduction of organic carbon, chemical oxygen demand (COD) measurements were also carried out to investigate the mineralization of the substrate using the open reflux method, according to standard procedures [11].

The energy consumption (EC) was calculated during the process according to [12]

$$\mathrm{EC} = \left[\frac{V I \Delta t}{\Delta \mathrm{COD}}\right] \quad (1)$$

EC is thus the energy consumption in kWh per kg COD reduced in the process (kWh/kg $\mathrm{COD_r}$); V is the cell potential in V, I is the current density in A, Δt is the electrolysis time in hours and ΔCOD is the amount of COD reduction during the time <DELTA> t, in kg.

The anode efficiency (AE) which is essentially the mass of reduced COD per unit of current passed through unit of surface area of anode per unit of electrolysis time (kg $\mathrm{COD_r}$/A $\mathrm{m^2}$ h), was also obtained from Eq. (2) [12].

$$\mathrm{AE} = \left[\frac{\Delta \mathrm{COD}}{I S \Delta t}\right] 10^{-6} \quad (2)$$

The apparent Faradic or current efficiency (CE) of COD removal can be calculated from [8]:

$$\mathrm{CE} = \left\{\frac{[(\mathrm{COD}_t) - (\mathrm{COD}_{t+\Delta t})]}{8 I \Delta t}\right\} F v \quad (3)$$

This parameter presents the percentage of total current consumed for eliminating COD in the samples, (COD_t) and ($\mathrm{COD}_{t+\Delta t}$) are the chemical oxygen demand at times t and $t+\Delta t$ (mg $\mathrm{O_2 L^{-1}}$) respectively, I is the current (A), F is Faraday's constant (26.8 Ah), and v is the volume of the treated wastewater (L), the numerical constant (8) taken into account the equivalent weight of O_2 due to the cathodic reactions [13]:

$$\mathrm{O_2 + 2H_2O + 4e^- \rightarrow 4OH^-} \quad (4)$$

$$\mathrm{O_2 + 4H^+ + 4e^- \rightarrow 2H_2O} \quad (5)$$

3. Results and discussion

3.1. The role of supporting electrolyte

Different salts were examined as supporting electrolytes (Na_2SO_4, $CaCl_2$, KCl, and NaCl) and the best one was chosen for use in the electrochemical process. At a constant potential of 5 V, different amounts of the salts were added to the electrolysis medium and the efficiency of dye removal was determined over 120 min. Using $CaCl_2$ at a concentration of 5 g $\mathrm{L^{-1}}$ resulted in considerable coagulation of the dye molecules. This prevented electrolysis and resulted in the failing of the electrodes and hence the salt was not investigated further.

There were no changes in UV–vis spectra of the dye solution during electrolysis in the presence of Na_2SO_4 as supporting electrolyte and this result was as the same as that observed when electrolysis of the dye solution was carried out in absence of electrolyte. Hence it appears that direct oxidation of the dye on the surface of anode is not important during electrolysis at 5 V. This finding is in agreement with other researchers' results [14] and hence this salt was not investigated further.

Fig. 4 shows the results obtained using NaCl and KCl as supporting electrolytes. It was observed that both electrolytes had considerable effect on the efficiency of dye degradation. Fig. 5 indicates that NaCl was the most effective supporting electrolyte, at an optimum concentration of 5 g $\mathrm{L^{-1}}$. By using this amount of NaCl, the dye removal per unit of consumed energy is higher than others. Also from the figure, it can be seen that there is a decrease in the amount of dye removal per unit of consumed energy by increasing the dye removal efficiency. It is due to this fact that with proceeding in the time of electrolysis, degradation of the dye molecules will lead to decolorization and also formation of several intermediates; consequent mineralization of these intermediates can also be occurred; therefore calculated EC is not only due to the decolorization process. The rest of experiments were carried out using 5 g $\mathrm{L^{-1}}$ of NaCl.

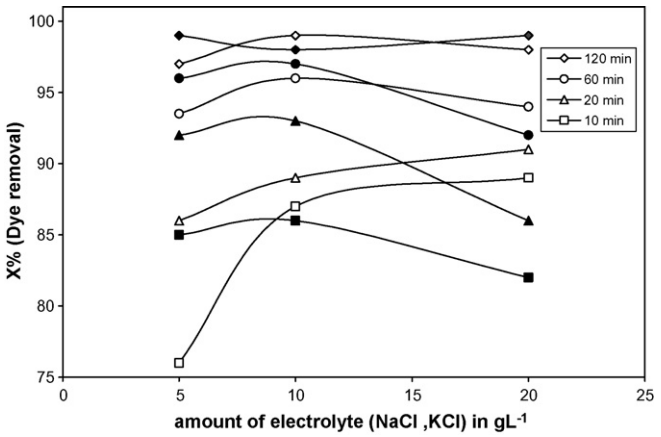

Fig. 4. Effect of supporting electrolytes on degradation of DB71 at different times. Black and white symbols present NaCl and KCl effect, respectively; $[DB71]_0 = 100\ \mathrm{mg\ L^{-1}}$, applied voltage = 5 V, initial pH 6.68. (Black symbols are for KCl and White symbols are for NaCl.)

Fig. 6 shows UV–vis spectra of the dye degradation collected during a 60 min electrolysis. In the visible region (λ_{max} = 584 nm) there is a rapid decrease in absorption due to azo bond cleavage in the dye molecules, the most active site for oxidation [15]. This shows that the electrochemical process is able to decolorize the dye solution in a short time. On commencing the process, absorption in the UV region increases up to 45 min and then decreases. This absorption increase may not be related to intermediate formation, because the absorption of OCl^- is also within this region, and hence may also have a role in this increase in absorbance. To investigate this, an aqueous solution of 5 g $\mathrm{L^{-1}}$ NaCl was electrol-

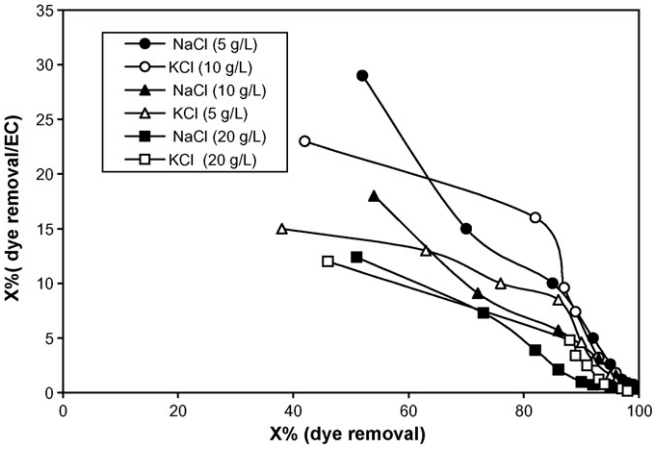

Fig. 5. Camparison chart for NaCl and KCl based on percentage of dye removal per unit of energy consumption verses of percentage of dye removal; $[DB71]_0 = 100\ \mathrm{mg\ L^{-1}}$, applied voltage = 5 V, initial pH 6.68.

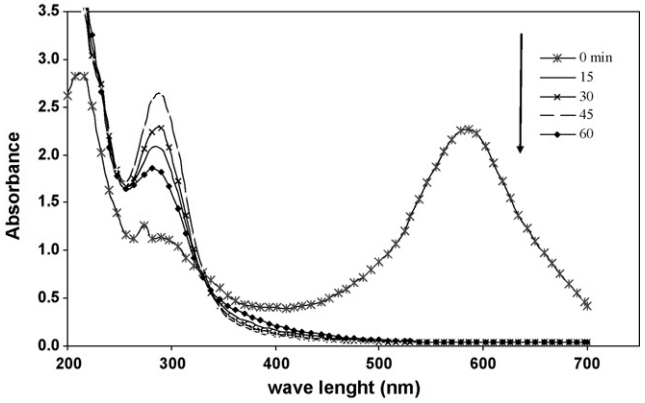

Fig. 6. UV–vis spectra changes of DB71 in aqueous media at different times; $[DB71]_0 = 100\,mg\,L^{-1}$, $[NaCl] = 5\,g\,L^{-1}$, applied voltage = 5 V, initial pH 6.68.

ysed at 5 V in the absence of dye, and the spectra so obtained are presented in Fig. 7. The results strongly suggest that the increase in UV absorption in Fig. 6 is due to the formation of OCl^-. In order to investigate the effect of electrolysis more closely, Chemical oxygen demand measurements were carried out, and the results are presented below.

3.2. Investigation the effect of applied voltage

3.2.1. The effect of voltage on COD removal

COD removal efficiencies were significantly affected by the cell voltage. The steady increase in %COD removal with cell voltage is in contact to other workers [8] who reported that the mineralization showed a maximum at 20 V. The results are presented in Fig. 8. At any time during electrolysis increasing the applied voltage was accompanied by an increase in the percentage of COD removal, presumably due to the increased generation of OCl^- species. After 120 min, the difference between the rate of conversions (%COD removal) for applied voltage of 15 and 20 V is just about 7%, which can not be an acceptable benefit for choosing 20 V potential as the best one since we are restricted in enhancing of potential by energy consumption consideration.

Fig. 9 shows that at any time during electrolysis, the pH increases above the starting value of 6.7. However at fixed cell voltage, this increase is last to same extend as the electrolysis proceeds due to consumption of hypochlorite anion in the degradation process.

The maximum variation in the pH is between the 0 to 5 V and in this range the lowest COD removal from the solution was observed. Therefore it may be concluded that, up to 5 V the accumulation of

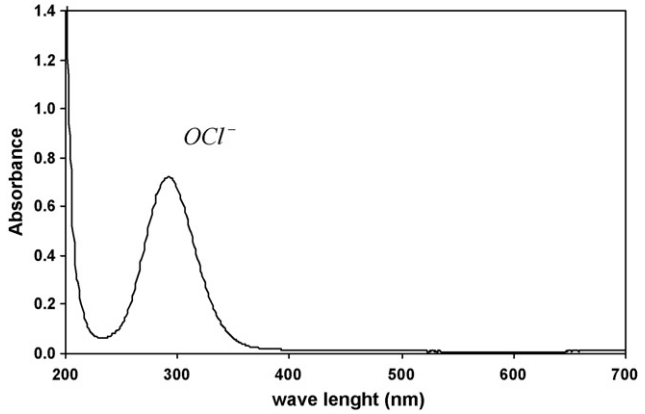

Fig. 7. UV–vis spectra of OCl^- in aqueous media.

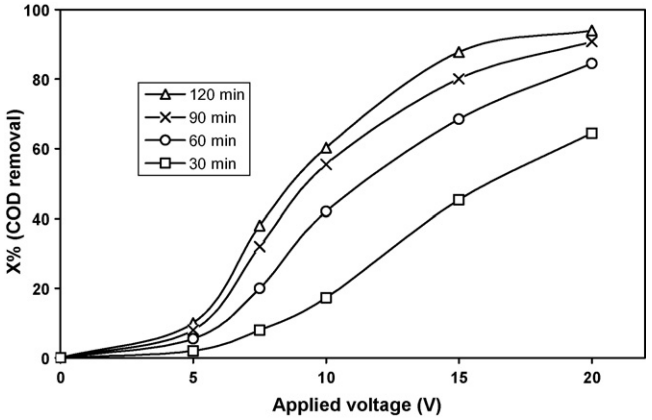

Fig. 8. Effect of applied voltage on amount of COD removal in different times; $[DB71]_0 = 100\,mg\,L^{-1}$, $[NaCl] = 5\,g\,L^{-1}$, initial pH 6.68.

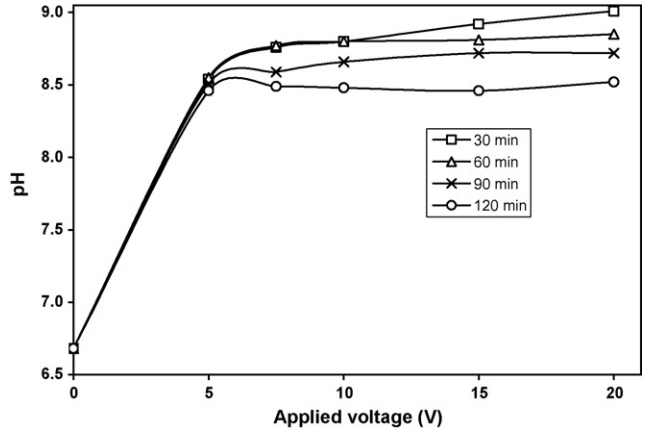

Fig. 9. Effect of applied voltage on pH of solution in different times; $[DB71]_0 = 100\,mg\,L^{-1}$, $[NaCl] = 5\,g\,L^{-1}$, initial pH 6.68.

OCl^- in the electrolyte causes the increase in pH after which the concentration of OCl^- reaches to a certain level at which point the oxidation process is initiated.

3.2.2. Determination of the optimum cell voltage based on current efficiency (CE)

Current efficiencies based on Eq. (3) were calculated and the results are presented in Fig. 10. The highest CE was observed at 15 V. Increasing the cell voltage from 15 to 20 V did not show a significant effect on COD removal (only 7%),

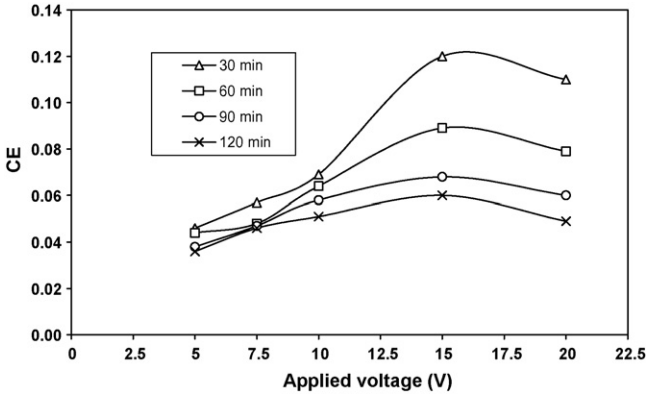

Fig. 10. Effect of applied voltage on current efficiency in electrochemical process at different times; $[DB71]_0 = 100\,mg\,L^{-1}$, $[NaCl] = 5\,g\,L^{-1}$, initial pH 6.68.

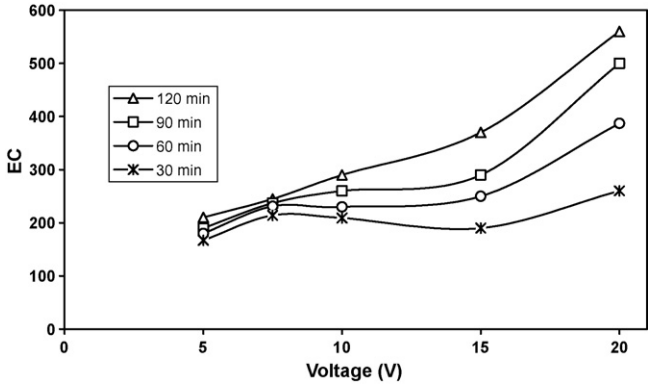

Fig. 11. Effect of applied voltage on energy consumption in electrochemical process at different times; $[DB71]_0 = 100\,mg\,L^{-1}$, $[NaCl] = 5\,g\,L^{-1}$, initial pH 6.68.

hence this was the cell voltage employed in subsequent experiment.

3.2.3. The effect of voltage on energy consumption (EC)

The energy consumption as a function of applied voltage was calculated and the results are shown in Fig. 11; it is clear from the figure that EC increases with voltage, but that these is a marked increase in EC between 15 and 20 V that is not reflected in COD removal (see Fig. 8), suggesting increased undesirable water electrolysis and demonstrating the importance of the choice of operating voltage.

3.3. Investigation the effect of pH

3.3.1. The effect of pH on COD removal

pH is another parameter that plays an important role in indirect electrochemical processes because it influences the form of the electrogenerated active chlorine and its oxidation potential [16]; thus, depending on the pH, the electrogenerated molecular chlorine can disproportionate to form hypochloric acid, see Eq. (6), which is deprotonate to hypochlorite ions, see Eq. (7).

$$Cl_2 + H_2O \rightarrow HOCl + H^+Cl^- \quad (6)$$

$$HOCl \rightarrow H^+ + OCl^- \quad (7)$$

For this study, pH of 4, 7 and 9 were selected. After adjusting the pH, electrolysis was commenced and the pH was kept constant at the desired value through the addition of 1 M H_2SO_4. The results are presented in Fig. 12.

The figure shows that the rate of COD removal increases slightly with increasing pH, due to the minimizing of the loss of active chlorine via gaseous chlorine leaving the cell or the formation of chlorate [17]. On the other hand, with increasing pH the oxidation potential of water decreases; leading to increased, undesirable water oxidation at the anode. The efficiencies observed at pH 7 and 9 are very similar and therefore identifying the optimum pH requires both CE and EC to be considered.

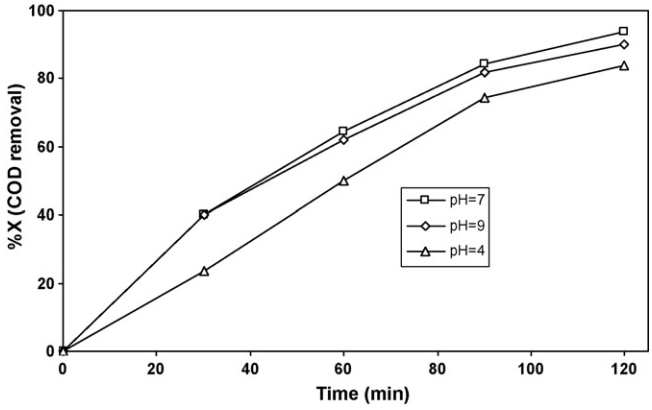

Fig. 12. Effect of pH on COD removal from DB71 solution during electrolysis times; $[DB71]_0 = 100\,mg\,L^{-1}$, $[NaCl] = 5\,g\,L^{-1}$, applied voltage = 15 V.

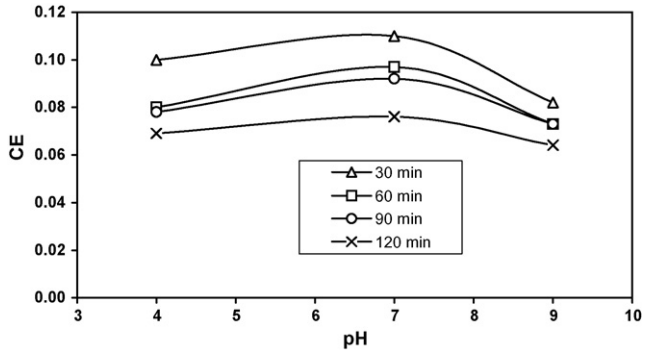

Fig. 13. Effect of pH on current efficiency in electrochemical process at different times; $[DB71]_0 = 100\,mg\,L^{-1}$, $[NaCl] = 5\,g\,L^{-1}$, applied voltage = 15 V.

3.3.2. Determination of the optimum pH based on CE and EC

From Figs. 13 and 14, it is clear that the CE and EC at pH 7 are maximum and minimum, respectively. Therefore pH 7 can be taken as the optimum pH. Lowest CE and highest EC at pH 9 can be due to the more favorable water oxidation condition. In the acidic solution low COD removal has been caused to low CE. At any pH the CE has been decreased by process progressing during the time and EC increased as well, which shows the enhancing in difficulty for oxidation of residual intermediates in the medium.

3.4. Kinetic investigations

In electrochemical oxidation, the rate of COD removal rate will be proportional to the pollutant and also chlorine/hypochlorite concentrations. Since pollutant removal taken place via indirect oxidation (when chloride is used as supporting electrolyte) the effect of chlorine/hypochlorite and therefore the kinetics of COD removal may be represented as [18]:

$$-d\frac{[COD]}{dt} = k[COD][Cl_2] \quad (8)$$

During electrolysis, chlorine/hypochlorite is produced by anodic oxidation of chloride, and it would be converted to chloride as the pollutant have been oxidized. Then the chloride would be anodically oxidized to form chlorine/hypochlorite, which oxidizes

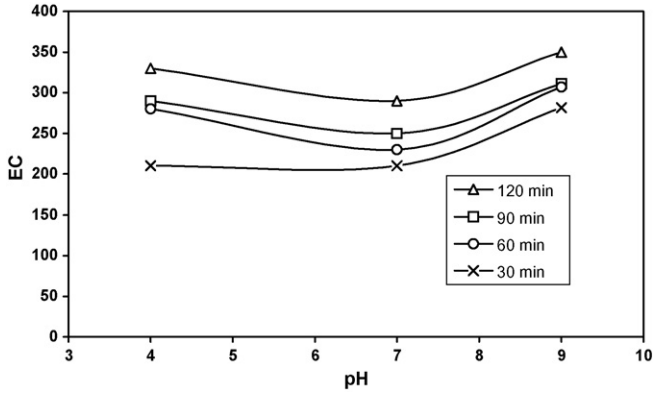

Fig. 14. Effect of pH on energy consumption in electrochemical process at different times; $[DB71]_0 = 100\,mg\,L^{-1}$, $[NaCl] = 5\,g\,L^{-1}$, applied voltage = 15 V.

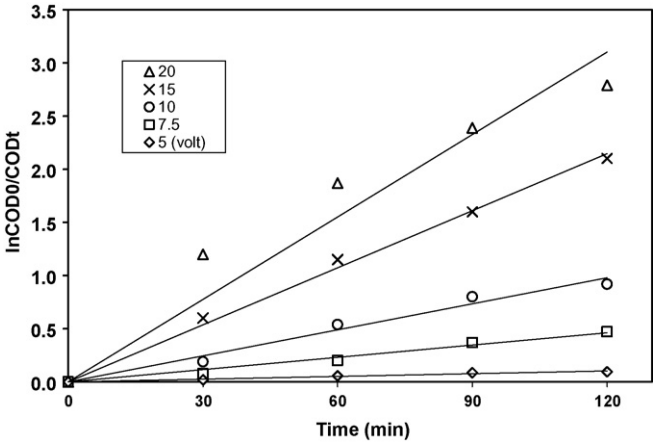

Fig. 15. Kinetic analysis for pseudo-first-order COD removal using different applied potential; $[DB71]_0 = 100\,mg\,L^{-1}$, $[NaCl] = 5\,g\,L^{-1}$, initial pH 6.68.

Table 2
Amounts of degradation rate constant of DB71 in different applied voltages in laboratory scale reactor.

Voltage (V)	5	7.5	10	15	20
k_{obs} (min^{-1})	0.0009	0.0039	0.0082	0.0179	0.0259

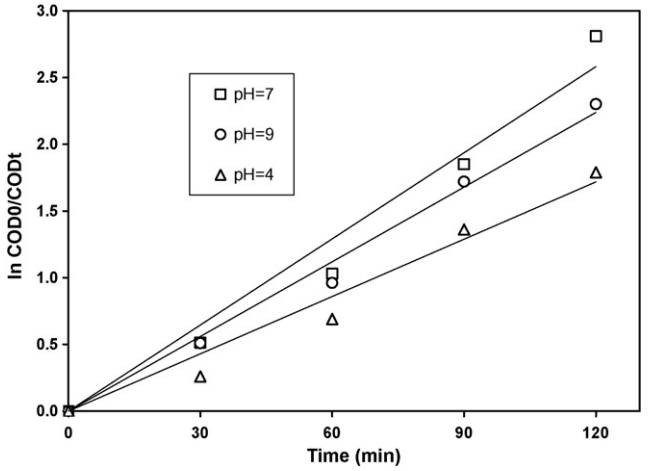

Fig. 16. Kinetic analysis for pseudo-first-order COD removal using different pH; $[DB71]_0 = 100\,mg\,L^{-1}$, $[NaCl] = 5\,g\,L^{-1}$, applied voltage = 15 V.

the pollutant again. Accordingly, the concentration of chlorine/hypochlorite can be assumed to be constant and $[Cl_2]$ and k in Eq. (8) may be merged into a pseudo-first-order kinetic constant (k_{obs}), see Eq. (9). By plotting $\ln [COD_0]/[COD_t]$ vs. time, k_{obs} can be obtained.

$$-d\frac{[COD]}{dt} = k_{obs}[COD] \quad (9)$$

The effect of applied potential and pH on the rate constant were investigated. The results are shown in Fig. 15 and Table 2, Fig. 16 and Table 3.

Table 3
Amounts of degradation rate constant of DB71 in different pH in laboratory scale reactor.

pH	4	7	9
k_{obs} (min^{-1})	0.0143	0.0215	0.0187

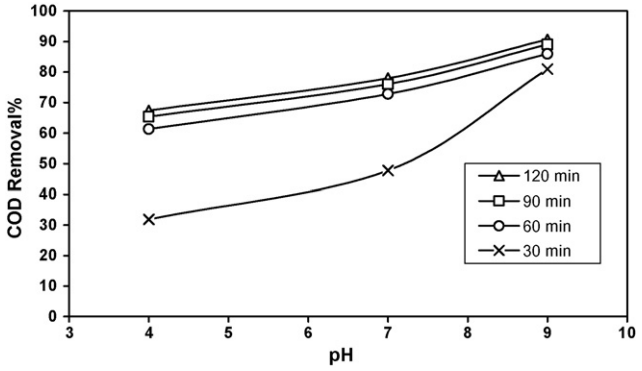

Fig. 17. Effect of pH on COD removal from DB71 solution using pilot scale reactor at different electrolysis times; $[DB71]_0 = 100\,mg\,L^{-1}$, $[NaCl] = 5\,g\,L^{-1}$, applied voltage = 15 V, initial pH 6.68 and $T = 25\,^{\circ}C$.

The results in the Table 2 show that voltage has an enhancing effect on rate constant because of the increase in concentration of active oxidant species such as Cl_2/OCl^- in solution.

Also it can be found that increasing the cell voltage from 15 to 20 V does not change the rate constant significantly meanwhile; the linearity trend of the plot has been weakened. This infers that under applied voltage of 20 V, the direct oxidation process can also have its appropriate role in electrochemical oxidation process simultaneously with indirect oxidation pathway. It therefore leads to weakness of validity for pseudo-first-order model. Fig. 16 and Table 3 show the effect of pH on the rate constant of dye mineralization. The kinetics of mineralization at all pH follow the first pseudo model and the highest rate constant was observed at pH 7, confirming the optimum pH as discussed above.

3.5. Pilot plant reactor

In order to investigate the applied aspect of process, a pilot plant scale reactor, described in Section 2.2 was utilized. For economic reason, two cheap and available stainless steel (304) electrodes were used in the reactor as anode and cathode.

Dye solutions with initial concentrations of $100\,mg\,L^{-1}$ in 9 L were prepared and transferred in to the reactor. COD removal was followed under the optimum conditions ($5\,g\,L^{-1}$ NaCl and cell voltage of 15 V) and at three pH 4, 7 and 9. The results showed that electrochemical oxidation, and also electro coagulation of the pollutant, took place in the pilot scale reactor. The coagulation leads to more efficient COD removal from solution, however it is in conflict with the aim of mineralizing pollutants and the prevention of sludge.

3.5.1. The effect of pH on COD removal

Fig. 17 shows that the highest COD removal (91%) was observed at pH 9, while COD removal at pH 4 was only about 65%. This may be due to the stability of $Fe(OH)_3$ coagulants in alkaline media which remove pollutants by adsorption. On the other hand, the OCl^- anions produced by the electrochemical oxidation process are more stable at pH 9, hence the higher COD removal efficiency.

By considering of 94% COD removal with lab cell reactor at operating pH condition of 7, it will be revealed that for achieving the same COD removal, operating pH should be increased and some coagulation must be appropriate. But for any sludge avoiding pH of media should be adjusted at acidic level and for achieving higher efficiency the time of electrolysis should be longer than 120 min.

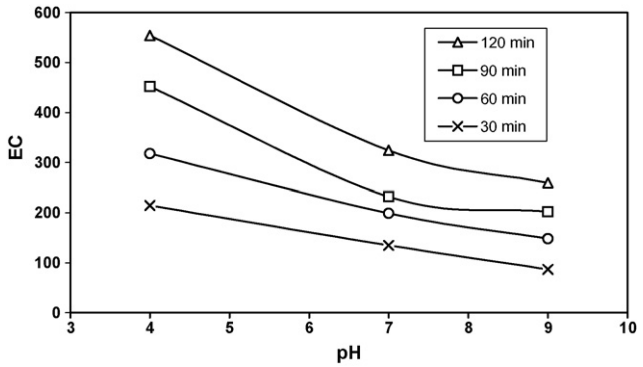

Fig. 18. Effect of pH on energy consumption in electrochemical process using pilot scale reactor at different electrolysis times; $[DB71]_0 = 100\,mg\,L^{-1}$, $[NaCl] = 5\,g\,L^{-1}$, applied voltage = 15 V, initial pH 6.68 and $T = 25\,^{\circ}C$.

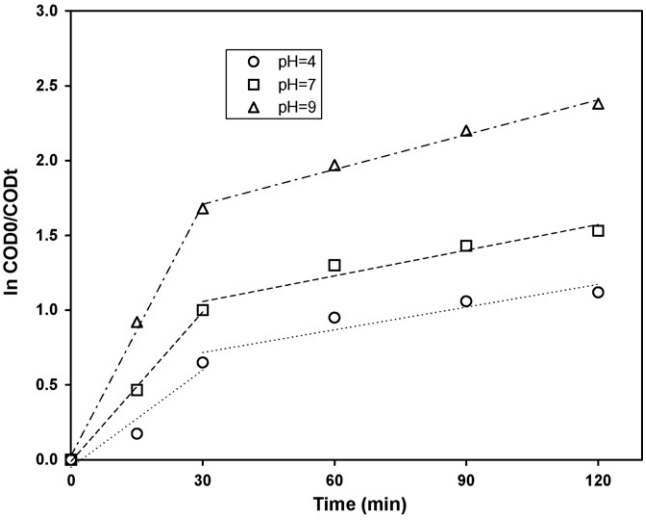

Fig. 19. Kinetic analysis for pseudo-first-order COD removal at different pH in pilot scale reactor; $[DB71]_0 = 100\,mg\,L^{-1}$, $[NaCl] = 5\,g\,L^{-1}$, applied voltage = 15 V and $T = 25\,^{\circ}C$.

3.5.2. The effect of pH on energy consumption (EC) and current efficiency (CE)

As it is obvious from the Fig. 18 the minimum energy consumption per unit of COD removal occurs at pH 9. The reason for this is the combination of electrochemical oxidation and electro coagulation in alkaline solution.

Fig. 19 shows the results of the kinetic investigations of electrochemical oxidation at pH of 4, 7 and 9. As it was shown in Section 3.4, the rate follow pseudo-first-order kinetics and the magnitude of the rate constants confirm the optimum pH for the process as pH 9.

Fig. 19 shows that, in the first 30 min of electrolysis, the COD depletion is a pseudo-first-order reaction and also shows that a pseudo-first order reaction might describe the behavior of the system over the 30–120 min period. However, in this case the values of rate constant (k) were about (4–7) fold lower compared with the first 30 min of the electrolysis (Table 4). This was probably due to the fact that during oxidation there is a formation of intermediates that are more difficult to remove. A similar behavior was observed by other researchers [19,20]. Thus it appears that there are differences in the mechanisms of electrolysis in the two reactors.

Table 4
Amounts of degradation rate constant of DB71 in different pH in pilot scale reactor.

pH	k_{0-30} (min^{-1})	k_{30-120} (min^{-1})
4	0.0197	0.0051
7	0.0329	0.0057
9	0.0571	0.0078

4. Conclusion

The present investigation illustrates the following results: (i) The most suitable conditions for degradation and mineralization of DB71 are: supporting electrolyte; NaCl with concentration of $5\,g\,L^{-1}$; neutral pH; and applied voltage of 15 V. (ii) Up to 15 V, indirect oxidation via hypochlorite is primary process. Hence the kinetics of COD removal shows a fit to a pseudo-first-order model. (iii) At 20 V, the direct oxidation of pollutants at the surface of the anode becomes important. (iv) The observed difference in the kinetics of COD removal in the two types of reactor may be due to some differences in intermediates produced during the electrochemical process. (v) For decolorization, at cell voltage of 5 V is adequate, but has negligible effect on mineralization. (vi) By using the lab scale reactor under optimum conditions complete mineralization obtained after about 120 min. (vii) The electrochemical oxidation process is promising with respect to the treatment of wastewaters containing azo dyes.

References

[1] A.G. Vlyssides, D. Papaioannou, M. Loizidoy, P.K. Karlis, A.A. Zorpas, Testing an electrochemical method for treatment of textile dye wastewater, Waste Manage. 20 (2000) 569–574.
[2] M.W. MacCurdy, D.G. Bordman, L.D. Michelsen, M.B. Woodby, Chemical reduction and oxidation combined with biodegradation for the treatment of a textile dye wastewater, in: Proc. 46th Purdue Ind. Waste Conf. Lafayette, 1992, pp. 229–234.
[3] J. Paprowicz, S. Slodczyk, Application of biologically activated sorptive columns for textile wastewater treatment, Environ. Technol. Lett. 9 (1988) 271–278.
[4] G. McKay, Color removal by adsorption, Am. Dyestuff Rep. 69 (1989) 38–45.
[5] M. Rossini, J. Garcia Garrido, M. Galluzzo, Optimization of the coagulation-flocculation treatment: influence of rapid mix parameters, Water. Res. 33 (1999) 1817–1826.
[6] M.A. Sanroman, M. Pazos, C. Cameselle, Optimization of electrochemical decolorization process of an azo dye, methyl orange, J. Chem. Technol. Biotechnol. 79 (2004) 1349–1353.
[7] J. Saein, A.R. Soleymani, Degradation and mineralization of Direct blue 71 in a circulating upflow reactor by UV/TiO_2 process and employing a new method in kinetic study, J. Hazard. Mater. 144 (2007) 506–512.
[8] Y. Xiong, P.J. Strunk, H. Xia, X. Zhu, H.T. Karlsson, Treatment of dye wastewater containing acid orange II Using a cell with three-phase three-dimension electrode, Water Res. 35 (2001) 4226–4230.
[9] J. Chen, M. Liu, L. Zhang, L. Jin, Application of nano TiO_2 towards polluted water treatment combined with electro-photochemical method, Water Res. 37 (2003) 3815–3820.
[10] T.C. An, X.H. Zhu, Y. Xiong, Feasibility study of photoelectrochemical degradation of methylen blue with three-dimensional electrode-photocatalytic reactor, Chemosphere 46 (2002) 897–903.
[11] APHA standard methods for examination of water and wastewaters, 17th ed., American Public Health Association, Washington, DC, 1989.
[12] A.G. Vlyssides, P.K. Karlis, N. Rori, A.A. Zorpas, Electrochemical treatment in relation to pH of domestic wastewater using Ti/Pt electrodes, J. Hazard. Mater. B95 (2002) 215–226.
[13] L. Szpyrkowicz, C. Juzzolino, N.S. Kaul, S. Daniele, D.M. De Fareri, Electrochemical oxidation of dyeing baths bearing disperse dyes, Ind. Eng. Chem. Res. 39 (2000) 3241–3248.
[14] M.A. Sanroman, M. Pazos, C. Cameselle, Optimization of electrochemical decolorization process of an azo dye, methyl orange, J. Chem. Technol. Biotechnol. 79 (2001) 1349–1353.
[15] Z. Sun, Y. Chen, Q. Ke, Y. Yang, Photocatalytic degradation of a cationic azo dye by TiO_2/bentonite nanocomposite, J. Photochem. Photobiol. A: Chem. 149 (2002) 169–174.
[16] G. Chen, Electrochemical technologies in wastewater treatment, Sep. Purif. Technol. 38 (2004) 11–41.
[17] M. Panizza, G. Cerisola, Electrochemical oxidation as a final treatment of synthetic tannery wastewater, Environ. Sci. Technol. 38 (2004) 5470–5475.
[18] D. Rajkumar, K. Palanivelu, Electrochemical treatment of industrial wastewater, J. Hazard. Mater. B113 (2004) 123–129.
[19] M. Panizza, G. Cerisola, Removal of organic pollutants from industrial wastewater by electrogenerated fenton's reagent, Water Res. 35 (2001) 3987–3992.
[20] R. Cossu, A.M. Palcaro, M.C. Lavagnolo, S. Palmas, F. Renoldi, Electrochemical treatment of landfill leachate: oxidation at Ti/PbO_2 and Ti/SnO_2 anodes, Environ. Sci. Technol. 32 (1998) 3570–3573.